

ACCEPTED MANUSCRIPT

## Angiogenic potential of spheroids from umbilical cord and adipose-derived multipotent mesenchymal stromal cells within fibrin gel

To cite this article before publication: Anastasiya Gorkun *et al* 2018 *Biomed. Mater.* in press <https://doi.org/10.1088/1748-605X/aac22d>

### Manuscript version: Accepted Manuscript

Accepted Manuscript is “the version of the article accepted for publication including all changes made as a result of the peer review process, and which may also include the addition to the article by IOP Publishing of a header, an article ID, a cover sheet and/or an ‘Accepted Manuscript’ watermark, but excluding any other editing, typesetting or other changes made by IOP Publishing and/or its licensors”

This Accepted Manuscript is © 2018 IOP Publishing Ltd.

During the embargo period (the 12 month period from the publication of the Version of Record of this article), the Accepted Manuscript is fully protected by copyright and cannot be reused or reposted elsewhere.

As the Version of Record of this article is going to be / has been published on a subscription basis, this Accepted Manuscript is available for reuse under a CC BY-NC-ND 3.0 licence after the 12 month embargo period.

After the embargo period, everyone is permitted to use copy and redistribute this article for non-commercial purposes only, provided that they adhere to all the terms of the licence <https://creativecommons.org/licenses/by-nc-nd/3.0>

Although reasonable endeavours have been taken to obtain all necessary permissions from third parties to include their copyrighted content within this article, their full citation and copyright line may not be present in this Accepted Manuscript version. Before using any content from this article, please refer to the Version of Record on IOPscience once published for full citation and copyright details, as permissions will likely be required. All third party content is fully copyright protected, unless specifically stated otherwise in the figure caption in the Version of Record.

View the [article online](#) for updates and enhancements.

## Angiogenic potential of spheroids from umbilical cord and adipose-derived multipotent mesenchymal stromal cells within fibrin gel

Gorkun A.A.<sup>1,2</sup>, Shpichka A.I.<sup>2</sup>, Zurina I.M.<sup>1,2</sup>, Koroleva A.V.<sup>3</sup>, Kosheleva N.V.<sup>1,4</sup>, Nikishin D.A.<sup>4,5</sup>, Butnaru D.V.<sup>2</sup>, Timashev P.S.<sup>2,6</sup>, Repin V.S.<sup>1</sup>, Saburina I.N.<sup>1</sup>

<sup>1</sup>*FSBSI Institute of general pathology and pathophysiology, Moscow, Russia*

<sup>2</sup>*Sechenov University, Institute for Regenerative Medicine, Moscow, Russia*

<sup>3</sup>*Laser Zentrum Hannover e.V., Hannover, Germany*

<sup>4</sup>*Lomosov Moscow State University, Faculty of Biology, Moscow, Russia*

<sup>5</sup>*Koltzov Institute of Developmental Biology of Russian Academy of Sciences, Moscow, Russia*

<sup>6</sup>*Federal Research Centre 'Crystallography and Photonics', Russian Academy of Sciences, Institute of Photonic Technologies, Moscow, Troitsk, Russia*

### Abstract

One of the essential goals in regenerative medicine is microvascularization which enables an effective blood supply within de novo constructed tissues and organs. In our study, we used two common multipotent mesenchymal stromal cell sources (subcutaneous adipose tissue and Wharton's jelly of the umbilical cord) where is a subpopulation of endothelial precursors. In the medium supplemented with VEGF, the 3D cultures of UC MMSCs and ADSCs promoted the endothelial cell differentiation. To evaluate their ability to form a capillary-like network, we encapsulated spheroids within non-modified and PEGylated fibrin hydrogels. The PEGylated hydrogel supported better the formation of multibranched cords than the pure fibrin gel. Analysis of tubule growth rate, length, and branching showed that the differentiated ADSCs had higher angiogenic potential than the differentiated hUC MMSCs. Our study can be a basis for the development of new strategies in tissue engineering and treatment of vascular diseases.

**Keywords:** spheroids, angiogenesis, vasculogenesis, mesenchymal stromal cells, fibrin, PEGylated fibrin

## Introduction

To date, one of the key issues in regenerative medicine is to find methods to form the vasculature within artificial tissues and organs that enables the biofabrication of vascularized grafts and prevention of acute and chronic ischemia causing their dysfunction. The main strategies applied to overcome this include the use of systems of *in vitro* and *in vivo* prevascularization, growth factors to stimulate blood vessel ingrowth, synthetic and decellularized materials with vascular architectonics, and integrated cellular components to enhance vascularization [1-3]. However, they are limited by the high tissue-engineered construct thickness which can cause hypoxia due to the insufficient vessel growth rate.

The new trend in this field is the fabrication of vascularized microtissues using 3D cultures of low differentiated cells [4, 5]. The spontaneous aggregation of multipotent mesenchymal stromal cells (MMSCs) in non-adhesive conditions leads to the spheroid formation, which attend the cell-cell interactions and formation of intercellular junctions [6], cell reprogramming to pluripotent cells [7, 8], synthesis of new extracellular matrix components, incl. tissue-specific proteins [9, 10], and active secretion of pro- and anti-inflammatory factors (interleukins, tumor necrosis factor, prostaglandins, etc.) [11]. In spheroids, cells are compacted and zoned into surface and central layers that causes emergent functional properties of the formed 3D modules. The surface cells form a dense layer and have adhesive intercellular junctions blocking diffusion that results in hypoxia within the central layer [12, 13]. Under these conditions, the cells in spheroids produce antihypoxic factors, which cause the resistance to apoptosis and increase the cell survivability after the transplantation into ischemic zones [14, 15]. However, when the spheroid diameter is more than 500  $\mu\text{m}$ , there is a necrotic core in its center [13]. Therefore, the optimal diameter of spheroids cultured in proangiogenic microenvironment is 150-200  $\mu\text{m}$  [16].

Thus, the MMSC spheroids are a promising tool for vascularization in regenerative medicine [9]. While previous studies on MMSCs and spheroids have mainly focused on cell behavior (e.g. the invasion and motility of ovarian cancer cell spheroids [17]), viability (testing new anti-cancer drugs [18]), survivability after the transplantation into ischemic zones [13, 16], development of hypoxia in 3D cultures [12, 19, 20], and *in vitro* angiogenesis modeling using only HUVEC (human umbilical vein endothelial cells) spheroids [21-23], none have discussed the possible use of the MMSC spheroids for the biofabrication of capillary-like structures within gels. And one of the most interesting gels to encapsulate the MMSC spheroids is fibrin gel, which is formed by catalytic fibrinogen cleavage caused by thrombin [24]. However, the application of pure fibrin is limited by its rapid degradation and opacity; and its chemical modification, e.g. PEGylation, is one of the possible ways to overcome these obstacles [24-26]. Moreover, it was shown that PEGylated fibrin hydrogels

1  
2 were able to stimulate angiogenesis [25, 26]. In this study, we therefore sought to reveal and  
3 compare the angiogenic potential of hUC MMSC (human umbilical cord MMSCs) and hADSC  
4 (human adipose-derived stromal cells) spheroids encapsulated within non-modified and PEGylated  
5 fibrin hydrogels.  
6  
7

## 8 9 **Materials and methods**

### 10 11 ***Primary cultures***

12  
13  
14 We used three samples of subcutaneous adipose tissue to isolate the stromal vascular fraction in  
15 accordance with standard procedures [27, 28]. All operations were performed under local  
16 anesthesia and aseptic conditions after a patient's signed informed consent. Briefly, we dissected  
17 the skin, separated the hypoderm from the abdominal wall muscles, and cut a fragment of the  
18 subcutaneous adipose tissue. These fragments were transported into sterile DMEM/F12 medium  
19 (1:1; PanEko, Russia) supplemented with gentamicin (400 U/mL, PanEko, Russia). We washed the  
20 samples with Hank's solution (BioLot, Russia) supplemented with antibiotics (gentamicin and  
21 penicillin/streptomycin) and then with fresh Hank's solution. We cut the tissue samples (<1mm),  
22 placed them into Petri dishes, and covered with DMEM/F-12 medium (1:1; PanEko, Russia)  
23 supplemented with L-glutamine (2 mmol/L; PanEko, Russia), basic fibroblast growth factor (bFGF,  
24 20 ng/mL; Prospec, Israel), gentamicin (50 µg/mL; PanEko, Russia), 1% insulin-selenite-transferrin  
25 (100×, BioloT, Russia), and 10% fetal calf serum (FCS, HyClone, USA).  
26  
27  
28  
29  
30  
31  
32  
33

34 To isolate hUC MMSCs, we used three umbilical cord samples after women signed an informed  
35 consent form. The primary culture of mesenchymal cells was obtained via the explant method. We  
36 transferred the umbilical cord samples from a transport container onto a sterile Petri dish filled with  
37 Hank's solution with antibiotics (100 U/mL penicillin and 100 µg/mL streptomycin) and washed.  
38 Then we cut them longitudinally, removed blood vessels, isolated Wharton's jelly, and mechanically  
39 minced it with scissors. The small Wharton's jelly fragments (<1 mm) were placed into Petri dishes  
40 and covered with DMEM/F-12 medium (1:1; PanEko, Russia) supplemented with L-glutamine (2  
41 mmol/L; PanEko, Russia), bFGF (20 ng/mL; Prospec, Israel), gentamicin (50 µg/mL; PanEko,  
42 Russia), 1% insulin-selenite-transferrin (100×, BioloT, Russia), and 10% FCS (HyClone, USA).  
43  
44  
45  
46  
47  
48  
49

### 50 51 ***Monolayer culture***

52 The cells were cultured under the standard conditions (37°C, 5% CO<sub>2</sub>). Every 2-3 days, we visually  
53 controlled cultures using a CKX41 inverted phase contrast microscope (Olympus, Japan) and  
54 changed the medium. Before passaging, the confluency of the cultures was 80%. The passage was  
55 carried out after incubating the cells in a mixture of 0.25% trypsin and EDTA (0.2 g/L in phosphate  
56  
57  
58  
59  
60

1 buffered saline (PBS) solutions (1:1) at 37°C for 1 minute. After passage 4, the cells were  
2 transferred into non-adhesive conditions.  
3  
4

### 5 **3D culture**

6 To prepare cell suspensions, both monolayer cultures (passage 4) were enzymatically treated with  
7 a mixture of 0.25% trypsin and EDTA (0.2 g/L in PBS) solutions (1:1). Then we centrifuged them (7  
8 min, 100 g), resuspended pellets in the growth medium to reach a concentration of  $3.3 \times 10^6$   
9 cells/mL, and placed into non-adhesive agarose plates prepared using 3D Petri Dish (Microtissue,  
10 USA). The filled agarose plates were transferred into 12-well plates (SPL, Korea). Cell  
11 differentiation in spheroids was induced by adding vascular endothelial growth factor A (VEGF A,  
12 Prospec, Israel) at a concentration of 10 ng/mL. Spheroids were cultured under the standard  
13 conditions (37°C, 5% CO<sub>2</sub>) in an incubator or in a special thermostatic chamber of a Cell-IQ device  
14 (CM Technologies, Finland) for live time-lapse microscopy. The growth medium was changed every  
15 2-3 days.  
16  
17  
18  
19  
20  
21  
22  
23  
24

### 25 **3D Angiogenesis assay**

26 To evaluate the spheroid ability to form a capillary-like network, we encapsulated them within non-  
27 modified and PEGylated fibrin hydrogels prepared as described elsewhere [25]. Briefly, fibrinogen  
28 was covalently bonded with polyethylene glycol (PEG) using O,O'-bis[2-(N-succinimidyl-  
29 succinylamino)ethyl]polyethylene glycol (PEG-NHS; Sigma-Aldrich, Germany) at a molar ratio 5 : 1  
30 (PEG-NHS : fibrinogen). The reaction mixture was placed into a thermostat (37°C) for 2h. The  
31 spheroid suspension was distributed in fibrinogen solution. The sufficient volume of thrombin  
32 solution was added (fibrinogen to thrombin ratio 1 mg to 0.2 U). This mixture immediately formed a  
33 gel. We monitored the process of tubule growth using a Cell-IQ device (ChipMan Technologies,  
34 Finland).  
35  
36  
37  
38  
39  
40  
41  
42

### 43 **Reverse-Transcription PCR**

44 Total RNA was isolated using TRI Reagent (Sigma, USA) according to manufacturer's instructions  
45 and treated with DNase I (Fermentas, USA) to remove the genomic DNA. One mg of RNA, M-MLV  
46 reverse transcriptase (Evrogen, Russia) and random hexanucleotides (Evrogen, Russia) were used  
47 for cDNA synthesis. PCR was performed on an MJ Mini amplifacator (BioRad) using Colored Taq-  
48 polymerase (Silex, Russia) and specific oligonucleotides (Evrogen, Russia) using the parameters  
49 that were selected considering the primer sequence and the product length. The forward and  
50 reverse primers for CD31 (PECAM-1, platelet/endothelial cell adhesion molecule 1) were 5'-  
51 ATGCGCAGGGATCTTTCTTAGTGG-3' and 5'-TAGGTCGGGCAGTGGGTTTCAGTTA-3',  
52  
53  
54  
55  
56  
57  
58  
59  
60

1  
2 respectively, and the forward and reverse primers for Flk-1 (vascular endothelial growth factor  
3 receptor 2) were 5'-AGCGGGGCATGTACTIONGACTGACGATTAT-3' and 5'-  
4 GGCGCACTCTTCCTCCAACACTG-3'. The forward and reverse primers for positive control gene,  
5 TATAA-box binding protein (TBP), were 5'-CATGACTCCCGGAATCCCTATCTTT-3' and 5'-  
6 TGTTGCTGCTGCTGCCTTTGTT-3', respectively. To exclude false-positive results, negative  
7 controls were included (PCR without reverse transcription and PCR without cDNA). The PCR  
8 products were analyzed using 1.5% agarose gel electrophoresis with ethidium bromide (0.5  
9 mg/mL). The primers were designed by Lasergene PrimerSelect (DNASTAR) using sequences  
10 from the NCBI GeneBank databases.  
11  
12  
13  
14  
15

### 16 17 ***Histology and Electron Microscopy*** 18

19  
20 To analyze the spheroid morphology, we fixed the samples with glutaraldehyde (3% in PBS; pH =  
21 7.4) for 1 hour at room temperature or overnight at +4°C. We washed the samples thrice with PBS  
22 and added OsO<sub>4</sub> (1% in PBS; pH 7.4) for 1 hour. Then they were washed thrice with PBS and  
23 dehydrated with ethanol (50% and 70%; twice for 5 min each). The samples were stored at +4°C in  
24 70% ethanol. For immunocytochemical analysis, monolayer cultures, spheroids, and tubule-like  
25 structures within gels were fixed in 4% paraformaldehyde (20 min, 4°C).  
26  
27  
28  
29

30 For transmission electron microscopy (TEM), the samples were further dehydrated with ethanol  
31 (80% – twice for 5 min; 96% – twice for 20 min; 100% – 20 min) and acetone (twice for 5 min). We  
32 prepared an epoxide resin consisting of Araldite GY, EMBED 812, DDSA and DMP30 catalyst  
33 (Electron Microscopy Science, USA) in advance and pre-incubated it for 1 hour at 37°C. After  
34 adding acetone, the samples were placed into closed tubes with a mixture of acetone and resin  
35 (1:1) for 1 hour at room temperature and then transferred into special dishes, which were filled with  
36 a pure resin for 1 hour at room temperature. To polymerize the resin, we incubated the samples at  
37 +60°C for 3-5 days. Ultrathin sections were made using a LKB-111 ultramicrotome (Sweden) and  
38 contrasted in 1% uranyl acetate in distilled water with lead citrate for 1 hour at room temperature in  
39 the dark [29]. The samples were studied using a JEM-1011 transmission electron microscope  
40 (JEOL Ltd., Japan).  
41  
42  
43  
44  
45  
46  
47  
48

49 To study the spheroid structure via scanning electron microscopy (SEM), we dried the samples at  
50 the critical point after fixation and dehydration. Then they were covered with gold in vacuum and  
51 studied using a CamScan-S2 scanning electron microscope (Cambridge Instruments, UK).  
52  
53

54 For immunocytochemical analysis, we washed the samples thrice with PBS (pH 7.4) for 5 min and  
55 incubated them overnight at +4°C with primary antibodies to endothelial markers (CD31, Flk-1,  
56  
57  
58  
59  
60

1 VEGF) and a mesenchymal marker (vimentin). The primary antibody solutions contained 0.15%  
2 Triton X-100 or 0.1% Tween 20 to increase the membrane permeability. The samples were washed  
3 with PBS (pH 7.4) and incubated for 1 hour at room temperature in the dark with the secondary  
4 goat-against-mouse antibodies conjugated with AlexaFluor488 and goat-against-rabbit antibodies  
5 conjugated to DyLight 594. Nuclei were stained with bis-benzimide (Hoechst 33258, Serva).  
6 Permanent mounts were prepared using VitroGel (Biovitrum, Russia) and analyzed in the visible  
7 and ultraviolet light using an Olympus Fluoview FV10I laser scanning confocal microscope  
8 (Olympus, Japan).  
9

### 10 **Flow cytometry**

11 Immunophenotyping of cells was carried out using a panel of markers – CD11b, CD14, CD34,  
12 CD31, CD45, CD73, CD90, and CD105. Aliquots of the cell suspensions were prepared using PBS  
13 (pH 7.4) supplemented with 1% fetal bovine serum (FBS). The samples were incubated in the dark  
14 (15 min, 25°C) with antibodies (10 µL of an antibody per 1 million cells) conjugated with fluorescent  
15 dyes (FITC – fluorescein isothiocyanate, PE – phycoerythrin). Then they were centrifuged (5 min,  
16 400 g) and resuspended in 1mL of PBS (pH 7.4) with 1% FBS. The analysis was performed using a  
17 Cytomics FC-500 flow cytometer (Beckman Coulter, Inc., USA).  
18

### 19 **Statistical analysis**

20 Our data was analyzed using STATISTICA 10 software. To compare four groups, we used the  
21 Kruskal-Wallis H-test, a nonparametric analogue of the one-way ANOVA test. To compare four  
22 groups, we used the Bonferroni correction for multiple comparisons;  $p < 0.05$  was considered  
23 statistically significant.  
24

## 25 **Results**

### 26 **Characterization of the monolayer and 3D cultures of UC MMSCs and ADSCs**

27 At passage 4, the monolayer cultures of UC MMSCs and ADSCs consisted of mesenchymal cells,  
28 which had fibroblast-like morphology (Fig. 1A, 2A) and expressed mesenchymal cell markers –  
29 vimentin and collagen type IV (Fig. 1B, 2B). Cell population analysis via flow cytometry revealed  
30 that in 2D conditions both cultures corresponded to the characteristics of multipotent mesenchymal  
31 stromal cells: the percentage of CD34 positive cells was below 5%; CD31 positive cells were  
32 absent; the number of CD90 and CD105 positive cells exceeded 95%. However, in the spheroids,  
33 there was an increase in the number of CD34 positive cells; the percentage of CD90/CD105  
34 positive cells was reduced; and CD31+ cells were still absent. These results showed that both cell  
35  
36  
37  
38  
39  
40  
41  
42  
43  
44  
45  
46  
47  
48  
49  
50  
51  
52  
53  
54  
55  
56  
57  
58  
59  
60

1  
2 cultures had a subpopulation of early endothelial progenitor cells, which spontaneously  
3 differentiated into CD34+ cells in the spheroids probably because of hypoxia. However, these  
4 conditions were not sufficient to obtain endothelial CD31+ cells (Table 1).  
5  
6

### 7 **VEGF induction of vasculogenesis in the spheroids**

8  
9  
10 We added VEGF, the main inducer of the endothelial cell differentiation and blood vessel growth, to  
11 the spheroids. After VEGF induction, the CD31+ cell population was detected in the spheroids that  
12 was concomitant with the CD105+ cell number reduction (Table 1). Using reverse transcription  
13 PCR, we showed that the expression of endothelial cell markers CD31 and Flk-1 (VEGF receptor)  
14 was upregulated in the cells from the spheroids. Immunocytochemical analysis also showed that in  
15 the spheroids the cells expressed endothelial markers CD31, Flk-1, and VEGF. Nevertheless, not  
16 all cells expressed endothelial markers CD31 and Flk-1; and some cells expressed a mesenchymal  
17 cell marker vimentin. Scanning electron microscopy (Fig. 3) revealed that within the VEGF-induced  
18 spheroids the cells formed cavities similar to capillary lumens that might be indicative of  
19 vasculogenesis.  
20  
21  
22  
23  
24  
25

### 26 **Encapsulation of the UC MMSC and ADSC spheroids within gels**

27  
28  
29 When we encapsulated the 7-day VEGF-induced spheroids within fibrin gels (Fig. 4, 5), the  
30 angiogenesis-type vessel growth was activated. While migrating, the cells formed branching cords,  
31 interconnected with each other. Around them, we observed the active mesenchymal cell migration  
32 from the spheroids. For our experiments, we used two gel types: non-modified (Supp. Video 1, 2)  
33 and PEGylated (Supp. Video 3, 4) fibrin hydrogels. The non-modified fibrin gel was more  
34 resorbable than PEGylated one. After the spheroid encapsulation, we noted that within the  
35 PEGylated fibrin hydrogel the cells formed more branched structures than those within the pure  
36 fibrin gel. The morphometric analysis of these structures was performed using Cell-IQ Analyzer  
37 analytical software, which can automatically determine tubules and calculate their length and the  
38 number of branch points. We found that the difference between these two cultures in tubule length  
39 and the number of branch points was significant only in the PEGylated fibrin gel (Fig.6, A, B). The  
40 average tubule growth rate for the VEGF-induced spheroids from UC MMSCs was 241.2  $\mu\text{m}/\text{day}$   
41 within the non-modified fibrin gel and 311.9  $\mu\text{m}/\text{day}$  within the PEGylated fibrin gel, from ADSCs –  
42 347.2  $\mu\text{m}/\text{day}$  within the non-modified fibrin gel and 615.3 within the PEGylated fibrin gel (Fig.6, C).  
43  
44  
45  
46  
47  
48  
49  
50  
51  
52  
53  
54  
55  
56  
57  
58  
59  
60

Table 1. Expression of surface markers in 2D and 3D UC MMSC and ADSC cultures

Marker	hUC MMSC			hADSC		
	2D culture	3D culture	3D culture + VEGF	2D culture	3D culture	3D culture + VEGF
CD11b	9.4%	2.2%	1.5%	1.2%	5.0%	3.2%
CD14	3.7%	5.0%	3.1%	1.1%	1.3%	1.7%
CD29	100.0%	100.0%	100.0%	99.2%	100.0%	100.0%
<b>CD31</b>	<b>0.0%</b>	<b>0.2%</b>	<b>31.9%</b>	<b>0.0%</b>	<b>0.5%</b>	<b>41.1%</b>
<b>CD34</b>	<b>1.5%</b>	<b>17.9%</b>	<b>1.7%</b>	<b>5.4%</b>	<b>12.2%</b>	<b>6.4%</b>
CD45	3.4%	0.8%	0.3%	9.1%	5.0%	0.7%
<b>CD90</b>	<b>94.9%</b>	<b>79.2%</b>	<b>74.4%</b>	<b>94.9%</b>	<b>76.7%</b>	<b>71.5%</b>
<b>CD105</b>	<b>99.3%</b>	<b>94.0%</b>	<b>28.3%</b>	<b>99.3%</b>	<b>98.3%</b>	<b>25.1%</b>

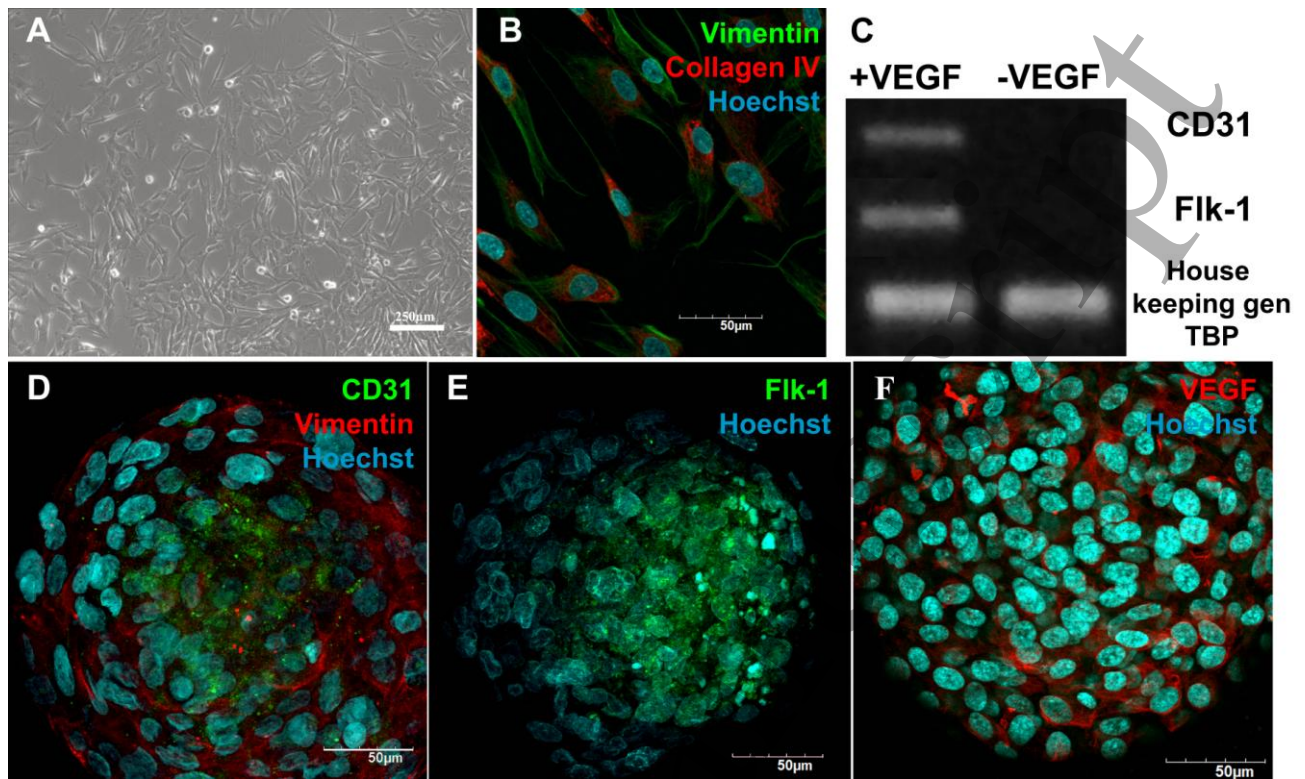


Figure 1. VEGF-induction of the endothelial differentiation in hUC MMSC spheroids. A. hUC MMSCs in the 2D culture, passage 4. *Phase contrast*. B. Expression of mesenchymal markers vimentin (green) and collagen type IV (red) in the 2D cell culture, passage 4; nuclei (blue) stained with Hoechst 33258. *Laser confocal scanning microscopy*. C. Expression of endothelial markers CD31 and Flk-1 after VEGF-induction. *Reverse transcription PCR*. D. Expression of an endothelial marker CD31 (green) and a mesenchymal marker vimentin (red); nuclei (blue) stained with Hoechst 33258. *Laser confocal scanning microscopy*. E. Expression of an endothelial marker Flk-1 (green); nuclei (blue) stained with Hoechst 33258. *Laser confocal scanning microscopy*. F. VEGF expression (red); nuclei (blue) stained with Hoechst 33258. *Laser confocal scanning microscopy*. Cell spheroids culture by day 7.

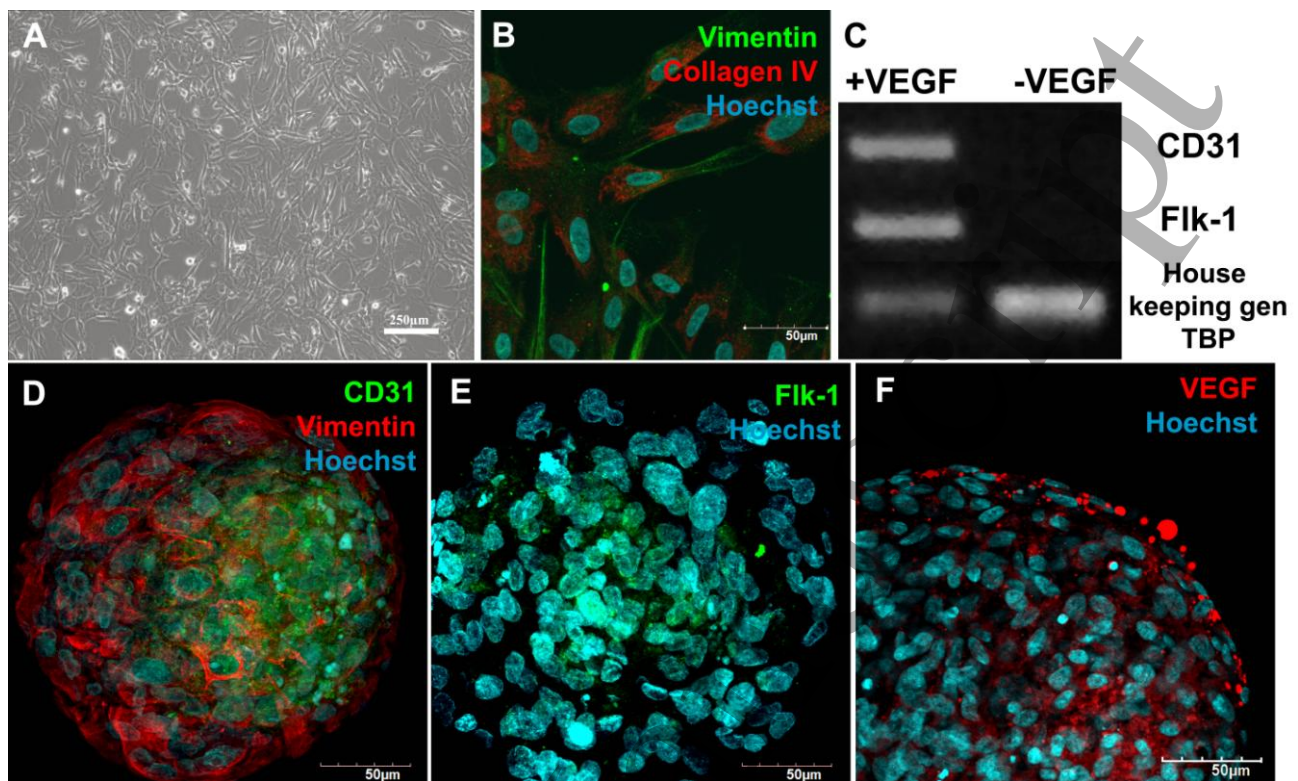


Figure 2. VEGF-induction of the endothelial differentiation in hADSC spheroids. A. hADSCs in the 2D culture, passage 4. *Phase contrast*. B. Expression of mesenchymal markers vimentin (green) and collagen type IV (red) in the 2D cell culture, passage 4; nuclei (blue) stained with Hoechst 33258. *Laser confocal scanning microscopy*. C. Expression of endothelial markers CD31 and Flk-1 after VEGF-induction. *Reverse transcription PCR*. D. Expression of an endothelial marker CD31 (green) and a mesenchymal marker vimentin (red); nuclei (blue) stained with Hoechst 33258. *Laser confocal scanning microscopy*. E. Expression of an endothelial marker Flk-1 (green); nuclei (blue) stained with Hoechst 33258. *Laser confocal scanning microscopy*. D. VEGF expression (red); nuclei (blue) stained with Hoechst 33258. *Laser confocal scanning microscopy*. Cell spheroids culture by day 7.

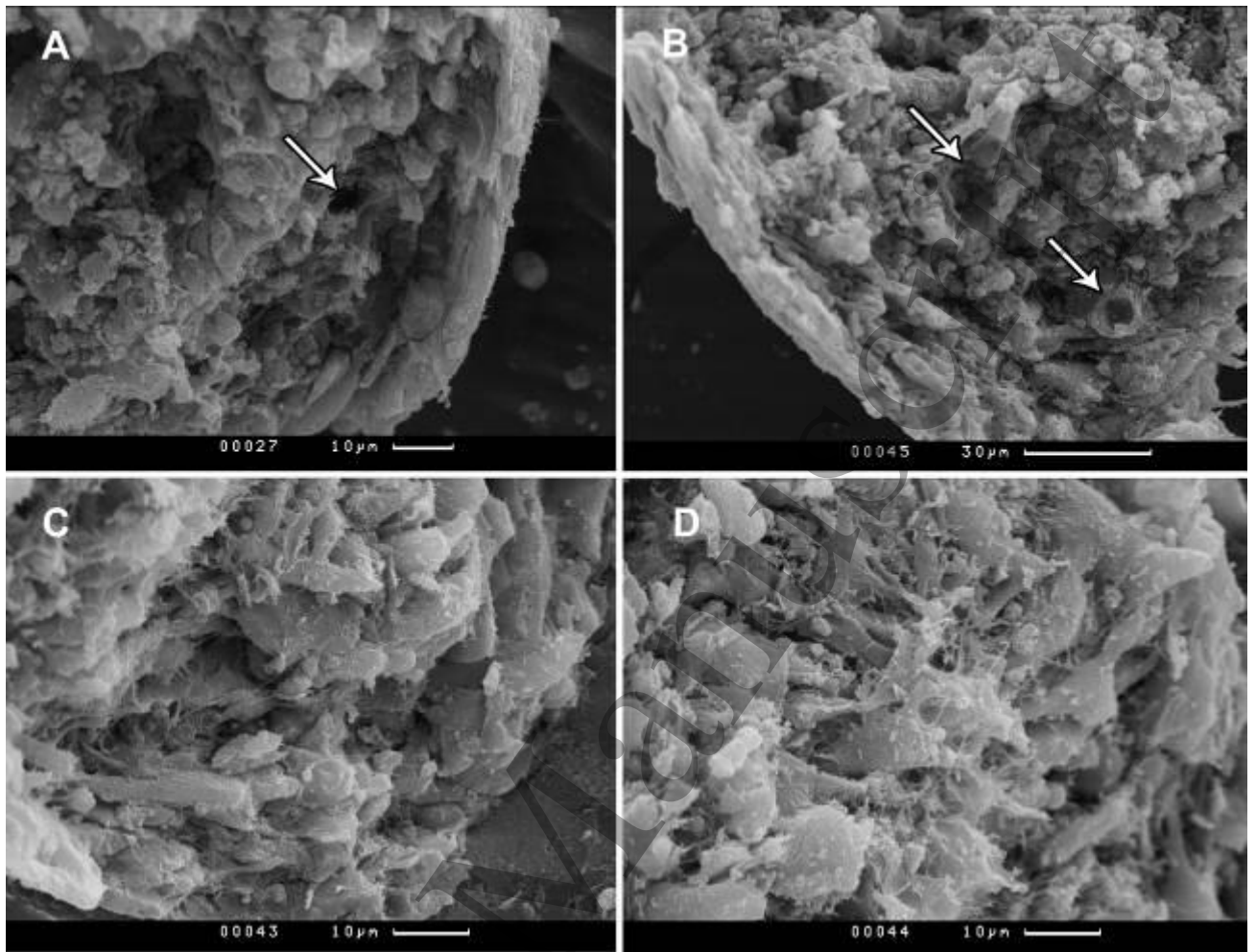


Figure 3. VEGF-induced lumenogenesis (arrows) within hUC MMSC (A) and hADSC (B) spheroids. Control: non-induced hUC MMSC (C) and hADSC (D) spheroids. *Scanning electron microscopy*. Cell spheroids culture by day 7.

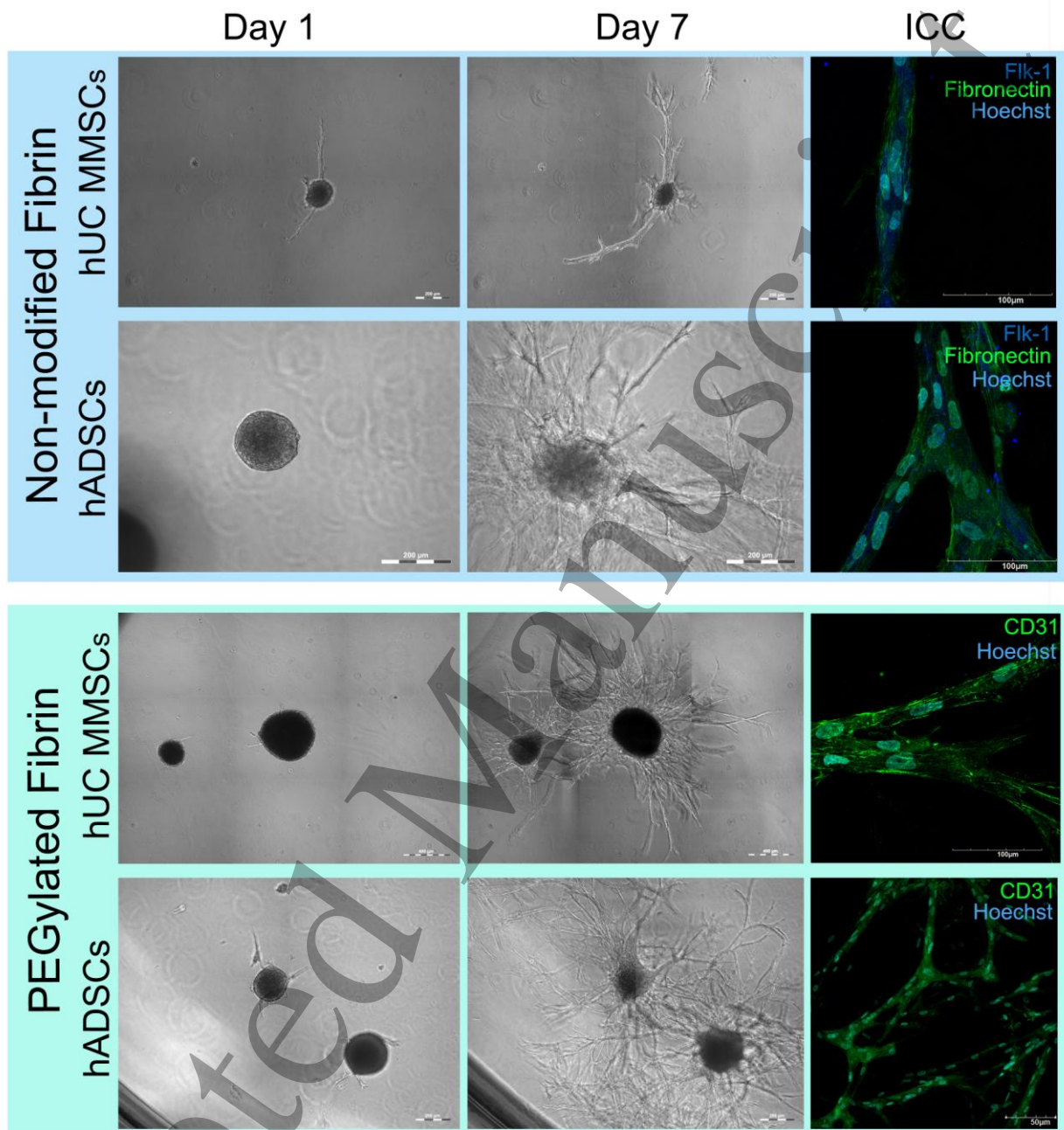
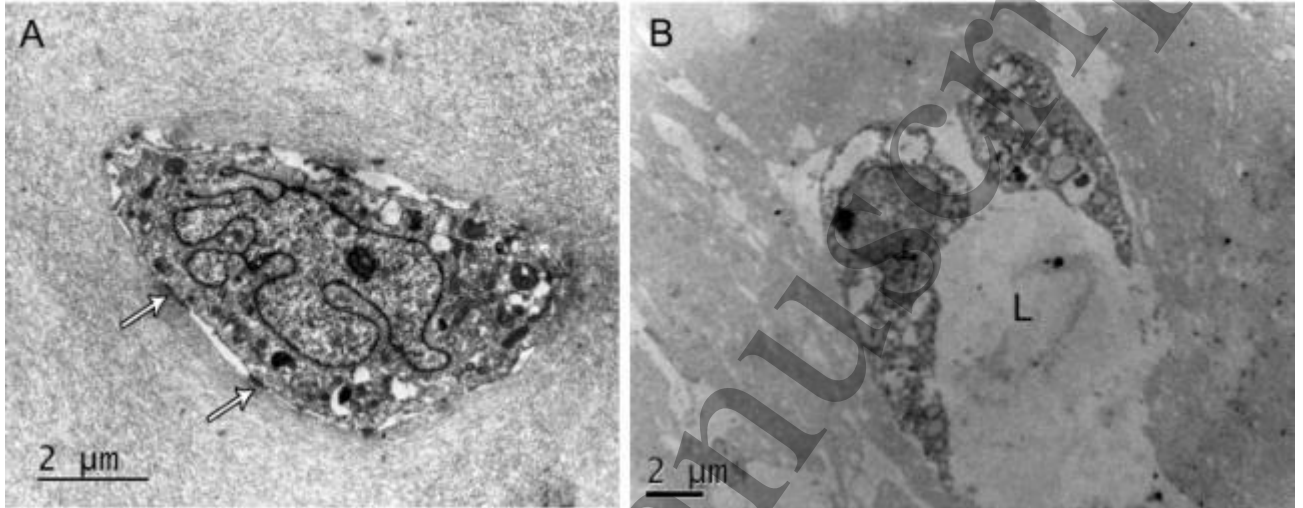


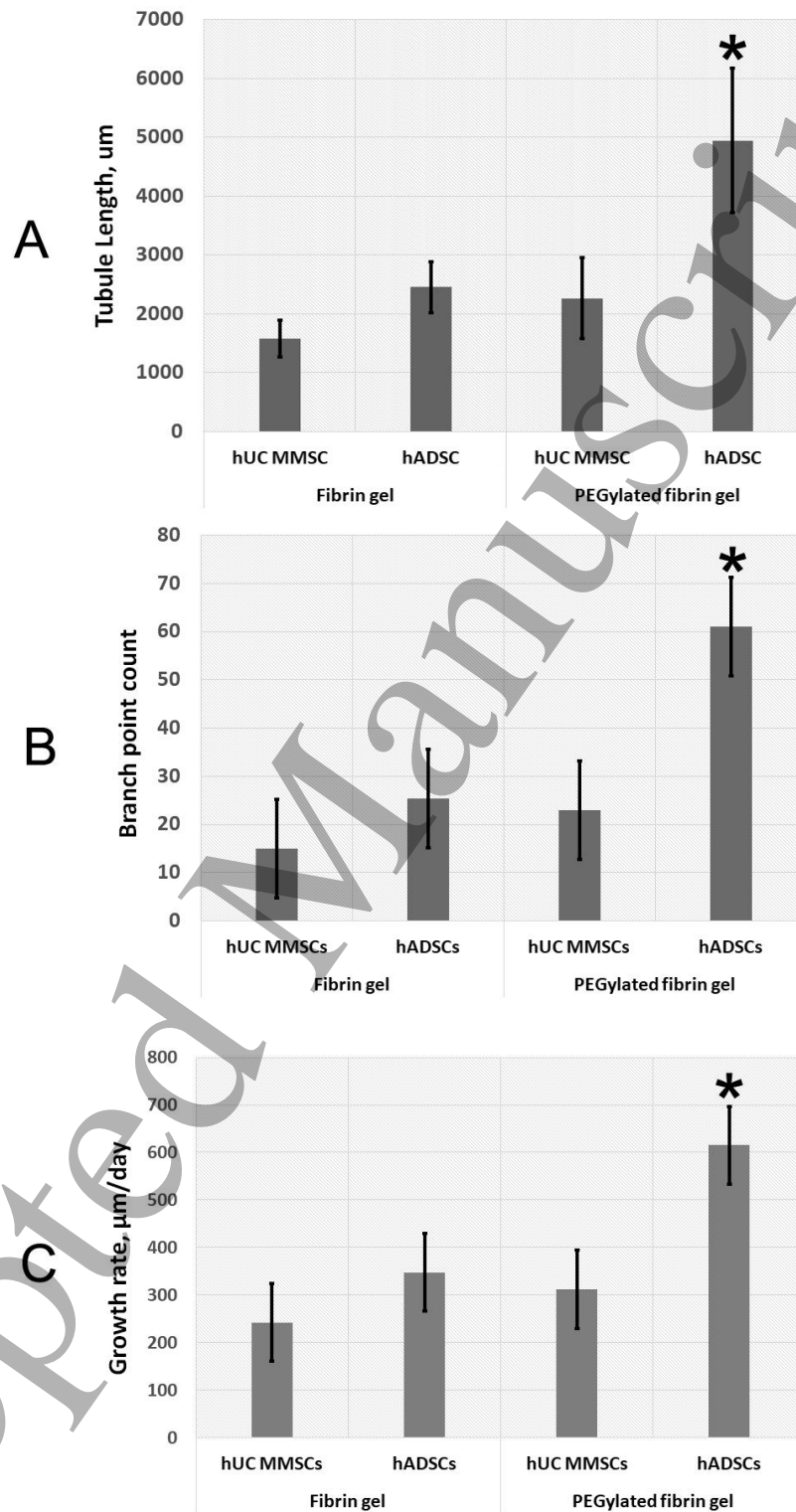
Figure 4. Angiogenesis assay of hUC MMSC and hADSC spheroids in the non-modified and PEGylated fibrin hydrogels.

UC MMSCs and ADSCs migrated from the spheroids during day 1 after encapsulation within the non-modified fibrin gel. By day 7, they formed low-branched cords (phase contrast, time-lapse microscopy) and synthesized an endothelial cell marker Flk-1 (dark blue) and an extracellular matrix protein – fibronectin (green). Nuclei (blue) stained with Hoechst 33258 (laser confocal scanning microscopy).

1  
2 UC MMSCs and ADSCs migrated from the spheroids during day 1 after encapsulation within the  
3 PEGylated fibrin gel. By day 7, they formed well-branched tubule-like cords (phase contrast, time-  
4 lapse microscopy) and synthesized an endothelial cell marker CD31 (green). Nuclei (blue) stained  
5 with Hoechst 33258 (laser confocal scanning microscopy).  
6  
7



25  
26  
27 Figure 5. Ultrastructure of sprouting cords growing from hUC MMSC spheroids within the non-  
28 modified (A) and PEGylated (B) fibrin hydrogels. A. Cross-section of a low-branched cord:  
29 migrating cell forms junctions (arrows) with the hydrogel. B. Cross-section of a tubule-like cord: the  
30 lumen formation (L) by polarized cells. *Transmission electron microscopy*.  
31  
32  
33  
34  
35  
36  
37  
38  
39  
40  
41  
42  
43  
44  
45  
46  
47  
48  
49  
50  
51  
52  
53  
54  
55  
56  
57  
58  
59  
60



53 Figure 6. Comparative analysis of the angiogenic potential of the VEGF-induced hUC MMSC and  
54 hADSC spheroids encapsulated within the non-modified and PEGylated fibrin hydrogels. A. Tubule  
55 length. B. Branch point count. C. Tubule growth rate. \*  $p < 0.05$ .

56  
57  
58  
59  
60

## Discussion

In this study, we compared the angiogenic potential of stromal cells from two accessible and ethically acceptable sources: the stromal vascular fraction from adipose tissue and Wharton's jelly from the umbilical cord. The main cell population isolated from these tissues was cell culture which had characteristics and properties of MMSCs [27, 30]. The obtained hADSC and hUC MMSC cultures corresponded to the MMSC characteristics accepted by the International Society for Cellular Therapy [31]: the cells had homogenous fibroblast-like morphology (Fig.1, 2, A) and CD105+/CD90+/CD45-/CD34-/CD14-/CD11b- immunophenotypic profile (Table 1, Supp.Fig. 1, Supp.Fig. 4) and expressed vimentin and collagen IV (Fig.1, B, Fig.2, B). Our data related to the lack of the endothelial marker CD31 and CD34 expression in the monolayer hADSC and hUC MMSC cultures (passage 4) (Table 1, Supp.Fig. 1, Supp.Fig. 4) is evidence of the absence of the spontaneous angiogenic induction in 2D conditions. Application of MMSCs from the umbilical cord and adipose tissue for vascularization and angiogenesis within tissue-engineered constructs [32, 33] is reasonable because both these cultures secrete proangiogenic factors [34-36] and contain subpopulations of cells competent to the endothelial differentiation [37, 38]. Therefore, to realize the potential of these progenitor cells, we need to activate them. To regulate proangiogenic and angiogenic potential, we can add proinflammatory factors to media [39, 40], create conditions for hypoxia [41], or influence the key signal cascades of angiogenesis [42].

The known facts about the vasculogenesis and angiogenesis regulation in ontogeny and pathological processes [43, 44] showed that microenvironment and tissue niche are significant for the realization of the differentiation potential of endothelial progenitor cells. Our approach to culture cells in non-adhesive 3D conditions and form cell spheroids allows us to create microenvironment for the realization of the cell differentiation potential in the conditions close to in vivo [6]. Within the spheroids from hADSCs and hUC MMSCs, there was the increase in CD34+ cell subpopulation – early endothelial progenitors; but the CD31+ endothelial-like cells were not revealed (Table 1, Supp. Fig. 2, Supp. Fig. 5). The increase in the CD34+ cell number might be caused by hypoxia in the spheroids, which is shown to occur in many papers [12, 19, 20], and enable the endothelial differentiation [45]. Therefore, the MSC cultivation in 3D conditions as spheroids led to the formation of microenvironment, which regulates the angiogenic potential of cells; but to activate their functional activity, we need to use an exogenous induction factor. As an induction agent, we choose VEGF A added to the growth medium. In the spheroids cultured with VEGF A, there was the subpopulation of the endothelial-like cells, which expressed CD31 (Table 1, Fig. 1, 2, C,D) and Flk-1 – VEGF receptor (Fig. 1, 2, C,E); but the cells that expressed a mesenchymal cell marker – vimentin – were still observed (Fig. 1, 2, D). Table 1 demonstrates that the maximum of the CD31+

1  
2 cells did not exceed 41% from all cells in the spheroids after VEGF-induction. This shows that not  
3 all cells in the spheroids were able for the terminal endothelial differentiation. Immunocytochemical  
4 staining confirmed the flow cytometry results: the cells expressing CD31 and Flk-1 were mostly  
5 located in the center of the induced hUC MMSC (Fig. 1, D, E) and hADSC (Fig.2, D, E) spheroids.  
6 The staining of the hADSC spheroids was brighter than that of hUC MMSC spheroids that indirectly  
7 shows the high sensitivity of the 3D hADSC culture to the inducing factor. Moreover, according to  
8 the flow cytometry data (Table 1, Supp. Fig. 3, Supp. Fig. 6), after VEGF-induction the CD90 and  
9 CD105 expression changed in the cells from both cultures. However, these changes were different.  
10 The CD90 expression slightly decreased that might be caused by the Thy1 expression in the  
11 endothelial cells [46]. At the same time, the number of the cells expressing CD105 did not exceed  
12 30% from all cells in the spheroids (Table 1, Supp. Fig. 3, Supp. Fig. 6) that showed the absence of  
13 the CD105 expression by the CD31+ cells. The same results were achieved for microvascular  
14 endothelial cells isolated from the human islets of Langerhans [47]. In general, the decrease in the  
15 number of the cells expressing CD90 and CD105 might be evidence of the additional non-revealed  
16 differentiation.

17  
18  
19  
20  
21  
22  
23  
24  
25  
26  
27 The VEGF expression common for endothelial and mesenchymal cells was revealed for all cells in  
28 the spheroids that is evidence of the angiogenesis autoregulation within a spheroid. Moreover,  
29 adding VEGF A induced the formation of lumens, which are typical for polar endothelial cells [48]  
30 (Fig. 3, A, B, arrows). Within the non-induced spheroids, the cells attached closely to each other;  
31 and there was no lumen (Fig. 3, C, D). This is evidence of the vasculogenesis within the spheroids  
32 caused by the high cell density and high density of signals among these cells. After VEGF-  
33 induction, the spheroids consisted of the mesenchymal and endothelial cell populations. Therefore,  
34 this induction stimulated the angiogenic differentiation only in the competent cells; and we were  
35 able to form the spheroid where were all necessary elements of the vessel wall (endothelial cells  
36 and cells capable of acting like mural cells and enhancing the angiogenesis). The spheroids with  
37 the mesenchymal cells and VEGF-induced subpopulations of the endothelial cells can be a unique  
38 material for the tissue engineering of vascularized microtissues.

39  
40  
41  
42  
43  
44  
45  
46  
47 To compare the spheroid angiogenic potential, we used two gel types: the non-modified and  
48 PEGylated fibrin gels. Both types are promising for clinical use due to their composition and the  
49 absence of xenogenic antigens and carcinogenic factors. However, the fibrin modification allowed  
50 us to change its mechanical and physicochemical properties (transparency and increase in gel  
51 density and its resistance to biodegradation). Shpichka et al. and Koroleva et al. [25, 26] showed  
52 that the PEGylated fibrin hydrogel supported vasculogenesis and angiogenesis during the 3D  
53 cultivation of HUVEC and hASC coculture. Within both gel types, the angiogenesis activation in the  
54  
55  
56  
57  
58  
59  
60

1 hUC MMSC and hADSC spheroids occurred during the first day (Fig. 4). By day 7, the  
2 encapsulated spheroids formed a primitive tubular-like network (Fig. 4), which consisted of the  
3 endothelial-like CD31+ (Fig. 4) and Flk-1+ (Fig. 4) cells and fibronectin-expressing mesenchymal  
4 cells (Fig.4) that mimics the blood vessel wall structure in vivo. However, the characteristics of this  
5 newly formed network were different depending on a gel type. Within the non-modified gel, the cells  
6 formed a cell thick low-branched tubular-like structure (Fig. 5, Fig. 6, B). Within the PEGylated fibrin  
7 gel, we observed the formation of interconnected multibranched capillary-like structures (Fig. 6, B)  
8 and lumens among the polar cells (Fig. 5). Moreover, within the PEGylated fibrin, the growth rate of  
9 the capillary-like structures was higher (Fig. 6, C) and the formed tubules were longer (Fig.5) than  
10 those within the pure fibrin. This might be caused by the fibrin modification with PEG-NHS that  
11 changed the gel micropatterning [26, 49] on an interface with the migrating cells and partially  
12 blocked the cell adhesion to fibrin fibers [50] that increased the cell migration and tubule growth.  
13 Thus, the change in the hydrogel structural properties permitted us to create a system of new cell  
14 interactions for the active collective cell migration, polarization, and lumenogenesis within the  
15 induced 3D ADSC culture. In general, the angiogenesis stimulation of the hADSC spheroids within  
16 the hydrogels was more effective than that of the hUC MMSC spheroids. This might be caused by  
17 individual sample features, their transport and cultivation conditions, and high number of tissue-  
18 specific cells competent to the angiogenic differentiation. Therefore, further study is required  
19 because the data on angiogenic properties of MMSCs isolated from different sources are  
20 discrepant [32, 51].

## 21 Conclusions

22 In our study, we showed that the hUC MMSC and ADSC cultures contained the cell subpopulation  
23 that can be stimulated to differentiate in the 3D culture. Because of the differences in tubule growth  
24 rate, length, and branching, the differentiated ADSCs had higher angiogenic potential than the  
25 differentiated hUC MMSCs. For maintaining angiogenesis, the PEGylated fibrin hydrogel was more  
26 stable and supported better the formation of multibranched cords than the non-modified fibrin gel.  
27 Therefore, our results can be used as a new approach for the neovascularization of artificial tissues  
28 and organs and treatment of vascular diseases (ischemic heart disease, chronic liver impairment,  
29 cardiac infarction, etc.).

## 30 Acknowledgements

31 This work was supported by the State Programme of the Presidium and Departments of RAS in the  
32 field of "Fundamental studies in medical science" (Programme code III.12; cell isolation and  
33 cultivation), and the Russian Science Foundation (18-15-00407; hydrogel preparation, fibrinogen  
34  
35  
36  
37  
38  
39  
40  
41  
42  
43  
44  
45  
46  
47  
48  
49  
50  
51  
52  
53  
54  
55  
56  
57  
58  
59  
60

modification, VEGF-induction of endothelial differentiation). Part of the work using the methods of electron microscopy was performed using the equipment of the Electron microscopy laboratory of the Lomonosov Moscow State University with the financial support of the Ministry of Education and Science of the Russian Federation.

## References

1. Liew A W L and Zhang Y 2017 *International Journal of Bioprinting*. **3(1)** 3-17
2. Dew L, MacNeil S and Chong C K 2015 *Regenerative medicine*. **10(2)** 211-224
3. Mukherjee S, Sriram P, Barui A K, Nethi S K, Veeriah V, Chatterjee S, et al. 2015 *Advanced Healthcare Materials*. **4(11)** 1722-1732
4. Todhunter M E, Jee N Y, Hughes A J, Coyle M C, Cerchiari A, Farlow J, et al. 2015 *Nature methods*. **12(10)** 975
5. Fennema E, Rivron N, Rouwkema J, van Blitterswijk C and de Boer J 2013 *Trends in biotechnology*. **31(2)** 108-115
6. Kubatiev A, Zurina I, Kosheleva N, Gorkun A, Saburina I and Repin V 2015 *Journal of Cytology & Histology*. **6(6)** 1
7. Cheng N-C, Wang S and Young T-H 2012 *Biomaterials*. **33(6)** 1748-1758
8. Huang G-S, Dai L-G, Yen B L and Hsu S-h 2011 *Biomaterials*. **32(29)** 6929-6945
9. Cesarz Z and Tamama K 2016 *Stem cells international*. **2016**
10. Kosheleva N V, Zurina I M, Saburina I N, Gorkun A A, Kolokoltsova T D, Borzenok S A, et al. 2015 *Patogenez*. **13(2)** 4-11
11. Ylöstalo J H, Bartosh T J, Coble K and Prockop D J 2012 *Stem cells*. **30(10)** 2283-2296
12. Dmitriev R I, Zhdanov A V, Nolan Y M and Papkovsky D B 2013 *Biomaterials*. **34(37)** 9307-9317
13. Lin R Z and Chang H Y 2008 *Biotechnology journal*. **3(9-10)** 1172-1184
14. Bhang S H, Lee S, Shin J-Y, Lee T-J and Kim B-S 2012 *Tissue engineering Part A*. **18(19-20)** 2138-2147
15. Bhang S H, Cho S-W, La W-G, Lee T-J, Yang H S, Sun A-Y, et al. 2011 *Biomaterials*. **32(11)** 2734-2747
16. Repin V, Saburina I, Kosheleva N, Gorkun A, Zurina I and Kubatiev A 2014 *Bulletin of experimental biology and medicine*. **158(1)** 137-144
17. Sodek K L, Ringuette M J and Brown T J 2009 *International journal of cancer*. **124(9)** 2060-2070
18. Vinci M, Gowan S, Boxall F, Patterson L, Zimmermann M, Lomas C, et al. 2012 *BMC biology*. **10(1)** 29
19. Okkelman I A, Foley T, Papkovsky D B and Dmitriev R I Yea. *Multi-Parametric Live Cell Microscopy of 3D Tissue Models*: Springer). p 85-103.
20. Dmitriev R I and Papkovsky D B Yea. *Neuronal Cell Death*: Springer). p 55-71.
21. Boucher J M, Clark R P, Chong D C, Citrin K M, Wylie L A and Bautch V L 2017 *Nature communications*. **8** 15699
22. Pfisterer L and Korff T 2016 *Angiogenesis Protocols*. 167-177
23. Heiss M, Hellström M, Kalén M, May T, Weber H, Hecker M, et al. 2015 *The FASEB Journal*. **29(7)** 3076-3084
24. Shaikh F M, Callanan A, Kavanagh E G, Burke P E, Grace P A and McGloughlin T M 2008 *Cells Tissues Organs*. **188(4)** 333-346
25. Shpichka A, Koroleva A, Deiwick A, Timashev P, Semenova E, Moiseeva I Y, et al. 2017 *Cell and Tissue Biology*. **11(1)** 81-87

26. Koroleva A, Deiwick A, Nguyen A, Narayan R, Shpichka A, Kufelt O, et al. 2016 *BioNanoMaterials*. **17(1-2)** 19-32
27. Dubois S G, Floyd E Z, Zvonic S, Kilroy G, Wu X, Carling S, et al. Yea. *Mesenchymal Stem Cells*: Springer). p 69-79.
28. Zuk P A, Zhu M, Mizuno H, Huang J, Futrell J W, Katz A J, et al. 2001 *Tissue engineering*. **7(2)** 211-228
29. Reynolds E S 1963 *The Journal of cell biology*. **17(1)** 208
30. Baksh D, Yao R and Tuan R S 2007 *Stem cells*. **25(6)** 1384-1392
31. Dominici M, Le Blanc K, Mueller I, Slaper-Cortenbach I, Marini F, Krause D, et al. 2006 *Cytotherapy*. **8(4)** 315-317
32. Edwards S S, Zavala G, Prieto C P, Elliott M, Martínez S, Egana J T, et al. 2014 *Angiogenesis*. **17(4)** 851-866
33. Semenov O and Breyman C 2011 *Open Tissue Eng Regen Med J*. **4** 64-71
34. Kuchroo P, Dave V, Vijayan A, Viswanathan C and Ghosh D 2014 *Stem cells and development*. **24(4)** 437-450
35. Aguilera V, Briceño L, Contreras H, Lamperti L, Sepúlveda E, Díaz-Perez F, et al. 2014 *PLoS one*. **9(11)** e111025
36. Rohringer S, Hofbauer P, Schneider K H, Husa A-M, Feichtinger G, Peterbauer-Scherb A, et al. 2014 *Angiogenesis*. **17(4)** 921-933
37. Szöke K, Beckstrøm K J and Brinchmann J E 2012 *Cell transplantation*. **21(1)** 235-250
38. Chen M-Y, Lie P-C, Li Z-L and Wei X 2009 *Experimental hematology*. **37(5)** 629-640
39. Zubkova E S, Beloglazova I B, Makarevich P I, Boldyreva M A, Sukhareva O Y, Shestakova M V, et al. 2016 *Journal of cellular biochemistry*. **117(1)** 180-196
40. Lopatina T, Bruno S, Tetta C, Kalinina N, Porta M and Camussi G 2014 *Cell Communication and Signaling*. **12(1)** 26
41. Efimenko A, Starostina E, Kalinina N and Stolzing A 2011 *Journal of translational medicine*. **9(1)** 10
42. Zavala G, Prieto C P, Villanueva A A and Palma V 2017 *Stem cell research & therapy*. **8(1)** 203
43. Chung A S and Ferrara N 2011 *Annual review of cell and developmental biology*. **27** 563-584
44. Chappell J C and Bautch V L. Yea. *Current topics in developmental biology*. 90: Elsevier). p 43-72.
45. Prado-Lopez S, Conesa A, Armiñán A, Martínez-Losa M, Escobedo-Lucea C, Gandia C, et al. 2010 *Stem Cells*. **28(3)** 407-418
46. Lin C-S, Xin Z-C, Dai J and Lue T F 2013 *Histology and histopathology*. **28(9)** 1109
47. Wheeler-Jones C, Clarkin C, Farrar C, Dhadda P, Chagastelles P, Nardi N, et al. 2013 *Diabetologia*. **56(1)** 222-224
48. Drake C J 2003 *Birth Defects Research Part C: Embryo Today: Reviews*. **69(1)** 73-82
49. Théry M 2010 *J Cell Sci*. **123(24)** 4201-4213
50. D'Arcangelo E and McGuigan A P 2015 *Biotechniques*. **58(1)** 13-23
51. Du W J, Chi Y, Yang Z X, Li Z J, Cui J J, Song B Q, et al. 2016 *Stem cell research & therapy*. **7(1)** 163